

# GHz photon-number resolving detection with high detection efficiency and low noise by ultra-narrowband interference circuits

Tingting Shi<sup>1,2,3</sup>, Yuanbin Fan<sup>1</sup>, Zhengyu Yan<sup>1</sup>, Lai Zhou<sup>1</sup>, Yang Ji<sup>2,3</sup>, and Zhiliang Yuan<sup>1,†</sup>

<sup>1</sup>Beijing Academy of Quantum Information Sciences, Beijing 100193, China

<sup>2</sup>Institute of Semiconductors, Chinese Academy of Sciences, Beijing 100083, China

<sup>3</sup>College of Materials Science and Opto-Electronic Technology, University of Chinese Academy of Sciences, Beijing 100049, China

**Abstract:** We demonstrate the photon-number resolution (PNR) capability of a 1.25 GHz gated InGaAs single-photon avalanche photodiode (APD) that is equipped with a simple, low-distortion ultra-narrowband interference circuit for the rejection of its background capacitive response. Through discriminating the avalanche current amplitude, we are able to resolve up to four detected photons in a single detection gate with a detection efficiency as high as 45%. The PNR capability is limited by the avalanche current saturation, and can be increased to five photons at a lower detection efficiency of 34%. The PNR capability, combined with high efficiency and low noise, will find applications in quantum information processing technique based on photonic qubits.

**Key words:** single photon avalanche diode (APD); photon number resolution (PNR); detection efficiency

**Citation:** T T Shi, Y B Fan, Z Y Yan, L Zhou, Y Ji, and Z L Yuan, GHz photon-number resolving detection with high detection efficiency and low noise by ultra-narrowband interference circuits[J]. *J. Semicond.*, 2024, 45(3), 032702. <https://doi.org/10.1088/1674-4926/45/3/032702>

## 1. Introduction

In recent years, single-photon detection (SPD) techniques have been widely used for weak light detection in the fields such as quantum information (quantum computation<sup>[1]</sup> and quantum communication<sup>[2]</sup>), optical time-domain reflectometer<sup>[3, 4]</sup>, fluorescence measurements<sup>[5, 6]</sup> and laser ranging<sup>[7, 8]</sup>. These applications often demand stringent performance requirements for single-photon detectors. For example, it is necessary to maintain both high detection efficiency and low dark count or/and afterpulse noise for quantum key distribution application<sup>[2]</sup>. Among different applications, there may be different focuses on count rate, spectral range, dead time, and timing jitter, and even the ability to resolve photon numbers<sup>[9, 10]</sup>.

Most SPDs are binary, i.e., they can discriminate between the absence (zero) or presence (one or more) of photons only, but cannot identify the exact number of photons incident upon the detector simultaneously. Solutions to achieve photon number resolution (PNR) include temporal<sup>[11, 12]</sup> or/and spatial multiplexing<sup>[13–15]</sup> of binary detectors. However, temporally multiplexed detectors have a lower count rate limit, while spatial multiplexing introduces deterioration in the signal-to-noise ratio. In addition to the above schemes, certain single-pixel SPDs were demonstrated to have intrinsic photon number resolution, such as visible light photon counters<sup>[16]</sup>, quantum dot field-effect transistors<sup>[17]</sup>, transition-edge sensors<sup>[11, 18]</sup>, InGaAs/InP and silicon avalanche pho-

todiodes (APDs)<sup>[19, 20]</sup>. For instance, during the early evolution of the avalanche, the avalanche current from an APD consists of constrained amplification noise and is proportional to the number of photons in the incident pulse, provided that the avalanche does not grow into saturation<sup>[21]</sup>. Under gigahertz gating and self-differencing technology<sup>[22]</sup>, individual InGaAs APD was first demonstrated to resolve up to four photons with no need for multiplexing in space or time<sup>[19]</sup>. Subsequently, Liang *et al.* reported that an InGaAs/InP APD is capable of resolving up to three photons with the 40% detection efficiency at 1 GHz<sup>[23]</sup>. Without the need for cryogenic cooling, the high efficiency and low noise GHz APD with PNR is a suitable choice for practical fiber quantum key distribution (QKD), quantum computing and quantum random-number generators.

We have recently developed a novel and simple readout circuit called the ‘ultra-narrowband interference circuit’ (UNIC)<sup>[24, 25]</sup>. The UNIC can reject the strong background capacitive response with little distortion to the avalanche signal. Thus, UNIC-APD exhibits excellent performance with high detection efficiency and low afterpulse noise. However, its PNR has yet to be demonstrated. Previously, InGaAs/InP APDs have been demonstrated to achieve PNR using the self-differencing technology<sup>[19, 26]</sup> or low-pass filtering technique<sup>[23]</sup>. In this paper, we demonstrate a 1.25 GHz gated InGaAs/InP APD with PNR capability by cascading two UNICs. Since the photon number distribution of laser obeys Poisson statistics, there will be multiple photons in the pulsed light even if highly attenuated. Here we report an UNIC-APD which could resolve the deterministic number of photons up to four, with the detection efficiency as high as 45%. The PNR capability is limited by the avalanche current saturation. By reducing the detection efficiency to 34% and thus postponing the

Correspondence to: Z L Yuan, [yuanzl@baqis.ac.cn](mailto:yuanzl@baqis.ac.cn)

Received 14 SEPTEMBER 2023; Revised 7 NOVEMBER 2023.

©2024 Chinese Institute of Electronics

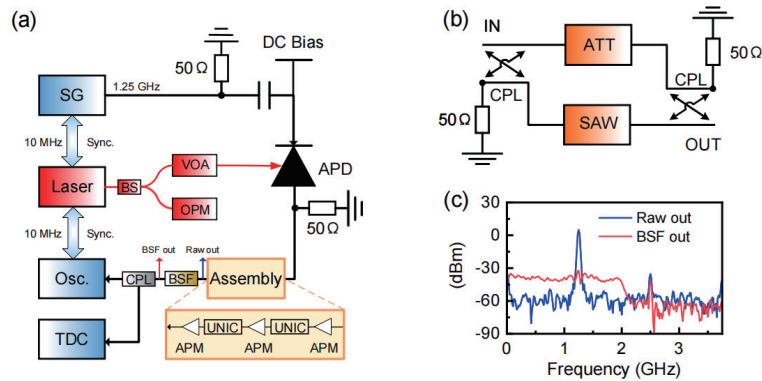


Fig. 1. (Color online) The photon-number resolving detection setup. (a) SG: signal generator; VOA: variable optical attenuator; APD: single-photon avalanche diodes based on InGaAs/InP; UNIC: ultra-narrowband interference circuits; BSF: band stop filter with a cut-off frequency of 2.5 GHz; APM: amplifier; OSC: oscilloscope; TDC: time-digital-converter. (b) Ultranarrow interference circuit (UNIC) consists of two couplers (CPL) with a power splitting ratio of 9 : 1, a  $\pi$ -resistance attenuator (ATT) and a surface acoustic wave band pass filter (SAW). (c) Transmission spectrum of raw out and BSF out.

avalanche saturation, we are able to increase its PNR capability to five photons.

## 2. Experimental set up

The photon-number resolving detection setup for APDs is depicted in Fig. 1(a). The APD was illuminated by a 1550 nm passively mode-locked femtosecond fiber laser, with a pulse repetition rate of 10 MHz and a pulse width of about 5–10 ps. The active area of the InGaAs/InP APD (Wooriro mini-flat) has a diameter of 25  $\mu\text{m}$ . According to our experimental requirements, the laser flux can be precisely controlled in the range of 0.01 to 100 photons/pulse using a variable optical attenuator (VOA, EXFO FTB-3500). The incident laser power is monitored in real time through a 50 : 50 beam splitter by an optical power meter (OPM, EXFO FTB-1750). The DC bias for the APD is provided by a source-measure unit (Keithley 2635B), which also measures the current flowing through the APD. The signal generator (SG, Tektronix AWG70000B) generates a 1.25 GHz sinusoidal gate signal, and the amplitude of gated voltage can be amplified up to 27  $V_{\text{pp}}$  continuously. The temperature of InGaAs/InP APD is regulated and stabilized at 30  $^{\circ}\text{C}$  by a temperature controller (Thorlabs TEC200). An appropriate DC bias is selected to match the sinusoidal gated voltage to achieve single-photon sensitivity at different detection efficiencies and temperatures.

The APD output is amplified before passing through an ultra-narrowband interference circuit (UNIC). UNIC is a RF Mach–Zehnder interferometer and consists of a  $\pi$ -resistance attenuator (ATT) and a surface acoustic wave band pass filter (SAW), as shown in Fig. 1(b). The power splitting ratio of two couplers is 9 : 1. The SAW is widely used in wireless communication<sup>[27]</sup>, which can effectively filter through just the capacitive response signal at the gating frequency  $f_{\text{gate}}$ . The processed signal transmitted through SAW interferes with the original signal attenuated by the ATT after a specified delay  $\Delta t$ , so as to produce destructive interference to reject  $f_{\text{gate}}$  signal and pass the avalanche signal. The UNIC differential delay ( $\Delta t$ ) can be expressed as  $\Delta t = (N_{\text{SAW}} + 1/2)/f_{\text{gate}}$ , where integer  $N_{\text{SAW}}$  is determined by the group delay caused by the SAW bandpass filter. In this experiment, we choose  $f_{\text{gate}} = 1.25$  GHz

and have  $N_{\text{SAW}} = 42$  and  $\Delta t = 34$  ns for precise frequency alignment. This long group delay relaxes the manufacturing precision requirement by a factor of 42 and enables small footprints of PCBs. It is possible to design the differential delay of SAW to match the APD gate frequency, which may facilitate development of faster and low-noise APDs in future. In order to achieve an optimal performance, three amplifiers (AMPs) of 6 GHz bandwidth and two identical 1.25 GHz UNICs are connected in series as an assembly in the circuit. The gains of the three AMPs are 15.5 dB (Mini-Circuits, ZX60-V62+, 0.05–6 GHz), 29 dB (SHF, S126 A, 80 kHz–25 GHz) and 29 dB (SHF, S126 A, 80 kHz–25 GHz). The AMPs are used to amplify the weak avalanche signal to be higher than the thermal noise and thus avoid avalanche signal distortion. Then, the avalanche signal passes through a band stop filter (BSF) with a cutoff frequency of 2.5 GHz in order to remove the second and high-order harmonic components of the transferred gate signal. Fig. 1(c) shows the frequency spectra of raw out (blue) and BSF out (red), which demonstrates that UNICs can effectively reject the strong capacitive response for a 1.25 GHz gating with little distortion of the avalanche signal.

Finally, the processed signal of the APD output is split by a RF coupler (CPL) into two paths, a high bandwidth oscilloscope (OSC, Keysight MXR404A, 4 GHz, 16 GS/s) and a time-digital-converter (TDC, Swabian Time Tagger Ultra). The laser provides a 10 MHz reference to SG, OSC and TDC. A large number of waveforms ( $5 \times 10^5$ ) collected by the oscilloscope are processed by computer programs to obtain the peak amplitude, peaking time, avalanche duration and integrated area of each avalanche.

## 3. Experimental results and discussion

Fig. 2(a) depicts the temporal evolution of the voltage distribution of avalanche signals for average detected flux of up to three photons/pulse. The voltage distribution varies at different time delays, as shown in Fig. 2(b). At a time delay of 0.11 ns (Fig. 2(b)), where the avalanche has not yet been triggered, the voltage distribution indicates the fluctuations of electrical noise. At a delay of 0.22 ns (green), where the avalanche begins, there are two peaks in the voltage distribution, at 0.018 and 0.16 V, representing 0-photon (electrical noise) and 1-photon, respectively. At a delay of 0.4 ns (red),

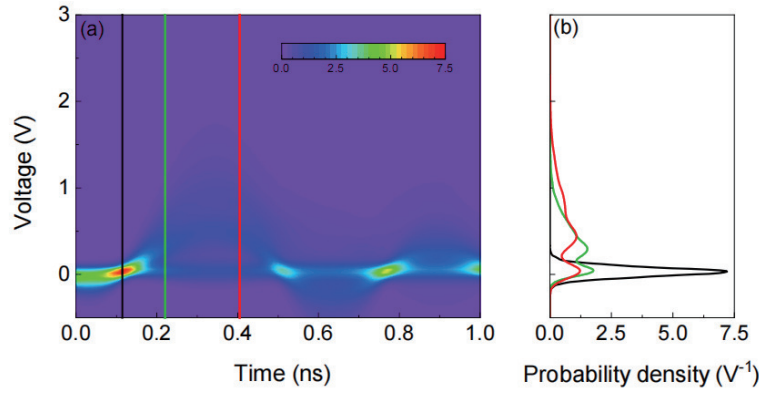


Fig. 2. (Color online) InGaAs/InP APD has intrinsic photon number resolution. (a) Temporal evolution of the avalanche peak voltage distribution for a detected flux of three photons/pulse. (b) The temporal voltage distribution at different time delays of 0.11 ns (black), 0.22 ns (green), and 0.4 ns (red), respectively.

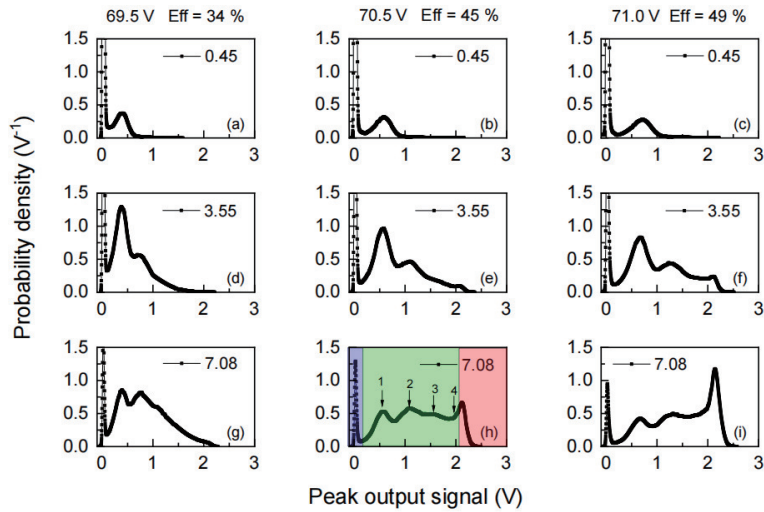


Fig. 3. (Color online) The evolution of peak output signal distribution measured for different voltage applied and incident photon fluxes on the APD. The bias voltages (detection efficiencies) of the three columns are 69.5 V (34%), 70.5 V (45%), and 71.0 V (49%), respectively. The incident photon fluxes in the three rows are 0.45, 3.55, and 7.08, respectively.

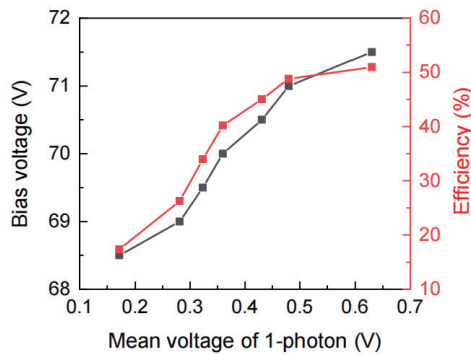


Fig. 4. (Color online) The bias voltage (black, left axis) and detection efficiency (red, right axis) vs. the mean voltage of one-photon peak voltage at a fixed photon flux  $\mu = 2.98$  photons/pulse.

where the avalanche is about to be quenched, yet the voltage distribution increases to three peaks, suggesting that the APD is able to resolve two photons under this bias condition. Photon number can also be discriminated through measuring the peak amplitude, peaking time, duration, or integration area of each avalanche<sup>[11]</sup>. For example, a higher number of photons detected in an avalanche, the stronger the avalanche amplitude or the longer the avalanche duration

and so on. After comparing different discriminating techniques, we find the peak amplitude is the most suitable to extract the photon number.

### 3.1. Qualitative explanation

Fig. 3 shows the evolution of peak output signal distribution measured for different voltage applied and incident photon fluxes on the APD. The bias voltages (detection efficiencies) of the three columns are 69.5 V (34%), 70.5 V (45%), and 71.0 V (49%), respectively. The incident photon fluxes in the three rows is 0.45, 3.55, and 7.08, respectively. Take Fig. 3(h) as an example:

- 1) The first peak at the voltage of 24 mV is the low electrical noise where no photons are detected (purple region).
- 2) The second peak centered at 0.56 V is the probability density distribution of one-photon detected and those at 1.09, 1.55, and 2.05 V correspond to  $N = 2, 3,$  and  $4$  photons, respectively (green region). That is, the number of simultaneously detected photons up to four photons with 45% detection efficiency.
- 3) At the last peak voltage, the avalanche signal is saturated. Saturation effect limits detector resolution (red region).

Fig. 4 demonstrates that the one-photon signal peak voltage increases with increasing bias voltage (detection effi-

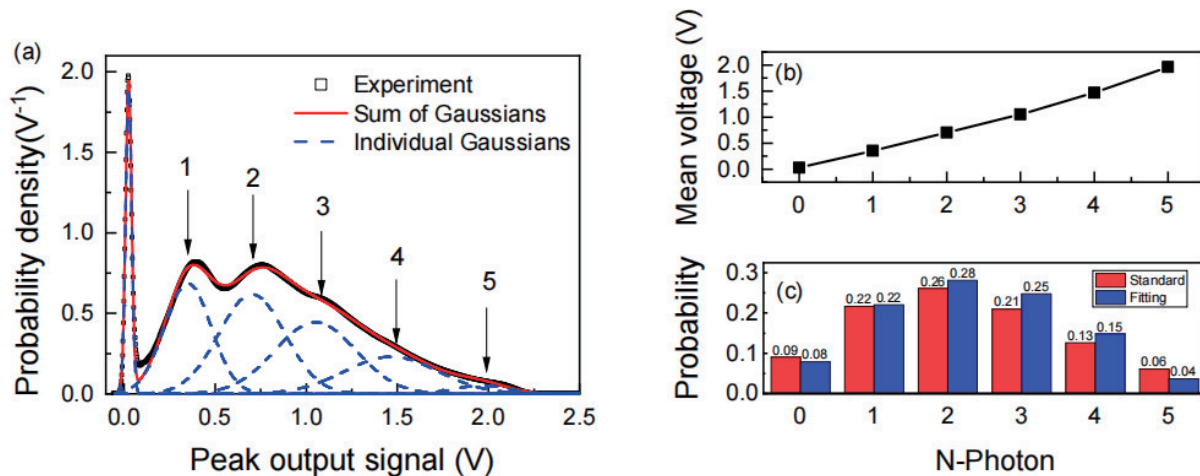


Fig. 5. (Color online) Quantitative analysis of photon number resolution for a detected flux  $\mu = 7.08$  photons/pulse. (a) Probability density distributions of avalanche peak voltages. The red solid line is a fit to the experiment data (symbols), indicating the sum of individual Gaussians (blue dashed line) of different photon numbers. (b) The mean voltage of peak output signal is proportional to the number of photons induced avalanches. (c) Comparison of the theoretical Poisson distribution (red) and the distribution of each photon number state of the APD (blue).

ciency) at a fixed photon flux  $\mu = 2.98$  photons/pulse. The trend is similar for other photon number states before saturation. According to Fig. 3 and Fig. 4, as the bias voltage increases, the ratio of the adjacent peak voltage separation to the standard deviation of one-photon-number state increases due to the higher avalanche gain, i.e., the capability of the photon number resolution improves, but the maximum number of distinguishable photons decreases due to the saturation effect.

### 3.2. Quantitative analysis

Fig. 5 presents the quantitative analysis of PNR for a flux  $\mu = 7.08$  photons/pulse and bias voltage 69.5 V. As the APD saturates faster at higher voltages (detection efficiency), the maximum number of resolvable photons decreases. Therefore, we chose a lower detection efficiency rather than a higher one, but it is also applicable at high efficiencies.

Fig. 5(a) shows the probability density distribution of avalanche peak voltages. The number of photons in the attenuated laser pulse obeys Poisson distribution, therefore, the data of avalanche height can be fitted with a Gaussian function with standard deviation (a Poisson distribution convolved with the energy resolution)<sup>[28]</sup>. Because of the statistical broadening due to avalanche noise, the width of the N-photon is scaled by  $N^{0.5}$  according to the width of the 1-photon. In addition, the width of 0-photon that reflects the fluctuation of electrical noise needs to be simulated separately. The red solid line in Fig. 5(a) represents the sum of individual Gaussians (blue dashed line) by modeling each photon number state with no other parameters, which agrees well with the probability density distribution of the experimental data (symbols).

The mean voltages of the individual Gaussians fitted in Fig. 5(a) are 0.029, 0.35, 0.70, 1.05, 1.46, and 1.96 V corresponding to  $N = 0-5$  photons, respectively. Fig. 5(b) indicates that the mean voltage of peak output signal is proportional to the number of photons induced avalanches before saturation.

The blue bar chart in Fig. 5(c) shows the distribution of different photon numbers detected by APD, which fits the theoretical Poisson distribution (red) with a detected mean photon number of 2.41. The probability distributions of the pho-

tons  $N = 1, 2, 3, 4$  are larger than the theoretical distribution, and we ascribe it to the afterpulse and fitting error. The discrepancy of the five-photon is because the distribution is no longer Gaussian due to the saturation effect.

In brief, the APD can resolve up to five photons with detection efficiency as high as 34% by appropriate assumptions and fitting.

## 4. Conclusion

In this article we have demonstrated the photon number resolution of InGaAs/InP single-photon avalanche photodiodes. With a simple, low-distortion ultra-narrowband interference circuit for the readout, 1.25 GHz gated avalanche photodiodes could resolve the number of simultaneously photons up to four photons with the detection efficiency of 45%. The high efficiency, low noise and high-count GHz avalanche photodiodes with photon number resolution capability will add to the existing toolbox enabling quantum information processing based on photonic qubits. The photon number resolution has also the potential to counter detector manipulation attacks in quantum key distribution<sup>[29]</sup>.

## Acknowledgments

The authors declare that there are no conflicts of interest related to this article. This work was supported by the National Natural Science Foundation of China (62250710162 and 12274406) and the National Key Research and Development Program of China (2022YFA1405100).

## References

- [1] Zhong H S, Wang H, Deng Y H, et al. Quantum computational advantage using photons. *Science*, 2020, 370(6523), 1460
- [2] Yuan Z L, Plews A, Takahashi R, et al. 10 Mb/s quantum key distribution. *J Lightwave Technol*, 2018, 36(16), 3627
- [3] Healey P. Optical time domain reflectometry—a performance comparison of the analogue and photon counting techniques. *Opt Quant Electron*, 1984, 16, 267
- [4] Li B, Zhang R, Wang Y, et al. Dispersion independent long-haul photon-counting optical time-domain reflectometry. *Opt Lett*,

- 2020, 45(9), 2640
- [5] Damalakiene L, Karabanovas V, Bagdonas S, et al. Fluorescence-lifetime imaging microscopy for visualization of quantum dots' endocytic pathway. *Int J Mol Sci*, 2016, 17(473), 1
- [6] Albertinale E, Balembois L, Billaud E, et al. Detecting spins by their fluorescence with a microwave photon counter. *Nature*, 2021, 600, 434
- [7] Wehr A, Lohr U. Airborne laser scanning-an introduction and overview. *ISPRS J Photogrammetry & Remote Sensing*, 1999, 54, 68
- [8] Li Z P, Ye J T, Huang X, et al. Single-photon imaging over 200 km. *Optica*, 2021, 8(3), 344
- [9] Hadfield R H. Single-photon detectors for optical quantum information applications. *Nature Photonics*, 2009, 3(12), 696
- [10] He T, Yang X, Tang Y, et al. High photon detection efficiency InGaAs/InP single photon avalanche diode at 250 K. *Journal of Semicond*, 2022, 43(10), 102301
- [11] Eaton M, Hossameldin A, Birrittella R J, et al. Resolution of 100 photons and quantum generation of unbiased random numbers. *Nature Photonics*, 2022, 17(1), 106
- [12] Natarajan C M, Zhang L, Coldenstrodt-Ronge H B, et al. Quantum detector tomography of a time-multiplexed superconducting nanowire single-photon detector at telecom wavelengths. *Optics Express*, 2013, 21(1), 893
- [13] Akiba M, Inagaki K, Tsujino K. Photon number resolving SiPM detector with 1 GHz count rate. *Opt Express*, 2012, 20(3), 2779
- [14] Cheng R, Zhou Y, Wang S, et al. A 100-pixel photon-number-resolving detector unveiling photon statistics. *Nature Photonics*, 2022, 17(1), 112
- [15] Huang K, Wang Y, Fang J, et al. Mid-infrared photon counting and resolving via efficient frequency upconversion. *Photonics Research*, 2021, 9(2), 259
- [16] Kim J, McKay K, Stapelbroek M, et al. Opportunities for single-photon detection using visible light photon counters. *Proc SPIE Advanced Photon Counting Techniques V*, 2011, 8033(1), 8033Q
- [17] Gansen E, Rowe M, Rosenberg D, et al. Single-photon detection using a semiconductor quantum dot, optically gated, field-effect transistor. *Conference on Lasers and Electro-Optics and Quantum Electronics and Laser Science Conference (CLEO/QELS)*, 2006, JTuF4
- [18] Lita A E, Miller A J, Nam S W. Counting near-infrared single-photons with 95% efficiency. *Optics Express*, 2008, 16(5), 3032
- [19] Kardynał B E, Yuan Z L, Shields A J. An avalanche-photodiode-based photon-number-resolving detector. *Nature Photonics*, 2008, 2(7), 425
- [20] Thomas O, Yuan Z L, Dynes J F, et al. Efficient photon number detection with silicon avalanche photodiodes. *Appl Phys Lett*, 2010, 97(3), 031102
- [21] Yuan Z L, Dynes J F, Sharpe A W, et al. Evolution of locally excited avalanches in semiconductors. *Appl Phys Lett*, 2010, 96(19), 191107
- [22] Yuan Z L, Kardynał B E, Sharpe A W, et al. High speed single photon detection in the near infrared. *Appl Phys Lett*, 2007, 91(4), 041114
- [23] Liang Y, Liu Z, Fei Q, et al. GHz Photon-number-resolving detection with InGaAs/InP APD. *Conference on Lasers and Electro-Optics (CLEO)*, 2019, JTu2A. 40
- [24] Fan Y, Shi T, Ji W, et al. Ultra-narrowband interference circuits enable low-noise and high-rate photon counting for InGaAs/InP avalanche photodiodes. *Optics Express*, 2023, 31(5), 7515
- [25] Yan Z, Shi T, Fan Y, et al. Compact InGaAs/InP single-photon detector module with ultra-narrowband interference circuits. *Adv Devices Instrum*, 2023, 4, 0029
- [26] Chen X, Wu E, Xu L, et al. Photon-number resolving performance of the InGaAs/InP avalanche photodiode with short gates. *Appl Phys Lett*, 2009, 95(13), 131118
- [27] Shao L, Zhu D, Colangelo M, et al. Electrical control of surface acoustic waves. *Nature Electronics*, 2022, 5(6), 348
- [28] Fukuda D, Fujii G, Numata T, et al. Photon number resolving detection with high speed and high quantum efficiency. *Metrologia*, 2009, 46(4), S288
- [29] Shen L, Kurtsiefer C. Countering detector manipulation attacks in quantum communication through detector self-testing. *European Conference on Optical Communication (ECOC)*, 2022, 1



**Tingting Shi** received the PhD degree from the Institute of Semiconductors, Chinese Academy of Sciences, Beijing, China, in 2023. Now she is an engineer at Beijing Academy of Quantum Information Sciences. Her current research focuses on single photon avalanche diodes.



**Zhiliang Yuan** received his PhD and post-doctoral training from the Institute of Semiconductors, CAS (1993–1997), and the University of Oxford (1997–2001), respectively. He then spent 20 years at Toshiba Cambridge Laboratory before returning to China in 2021 and serving as Chief Scientist at Beijing Academy of Quantum Information Sciences. He is known for high-speed quantum key distribution and electrically driven single-photon sources.